Journal of Sound and Vibration (2000) **235**(5), 863–873
doi:10.1006 jsvi.1998.2140, available online at http://www.idealibrary.com on IDEAL®

LETTERS TO THE EDITOR

A SELF-SENSING TECHNIQUE FOR ACTIVE ACOUSTIC ATTENUATION

D. J. Leo

Mechanical Engineering Department, Virginia Polytechnic Institute and State University, Blacksburg, VA 24061, *U.S.A.*

AND

D. Limpert

Mechanical, Industrial and Manufacturing Engineering Department, The University of Toledo, Toledo, OH, U.S.A.

(*Received* 2 *September* 1998, *and in final form* 8 *December* 1998)

1. INTRODUCTION

Active noise control has long been studied as a means of increasing the sound attenuation properties of materials and structures. The use of secondary sources for destructive interference of sound waves was experimentally demonstrated over 40 years ago [1, 2] but it wasn't until recently that advances in digital signal processing made active noise cancellation practical [3]. Continuing advances in digital signal processing technology have enabled the use of active noise control in several practical applications [4, 5].

A number of active control techniques utilize speakers and microphones as control elements. In the early work by Olson and May, an "electronic sound absorber" was developed from a microphone placed in close proximity to the cone of an enclosed loudspeaker [1]. Reductions in the sound pressure were obtained by feeding back the pressure measurement through an analog circuit to the loudspeaker input. More recently, Nelson and his colleagues developed multi-channel control algorithms for active sound absorption and adaptive control implementations have been studied by Nelson and Elliot [6], Nelson *et al.* [7], Elliot *et al.* [8] and Orduna-Bustamante and Nelson [9]. In all of the works cited above, acoustic pressure and mechanical velocity were the variables utilized in the control algorithms. As pointed out by Elliot, *et al.* [5], algorithms that utilize pressure and velocity as control variables result in power absorption. Optimal power absorption is achieved by matching the impedance of the electrical system to the impedance of the acoustic system with a feedback or feedforward compensator [8].

These works illustrate the utility of measuring acoustic pressure and velocity for active noise control. In this work, a "self-sensing" technique is developed in which the acoustic pressure and velocity are measured simultaneously from measurements of speaker voltage and current. Unlike previous research, in which these quantities were measured using microphones and accelerometers, the technique derived in this paper enables the measurement of pressure and velocity without the need for additional sensors. In addition to eliminating the need for hardware in the control system, this technique

0022–460X/00/350863 + 11 $35.00/0

enables the measurement of signals that are perfectly collocated with one another. Collocation has advantages in the development of dissipative feedback control laws.

The technique is motivated by previous research in the simultaneous sensing and actuation of flexible structures. The term "self-sensing" was introduced by Dosch *et al.* in their use of peizoelectric materials for the control of resonant modes in a flexible structure [10]. They demonstrated active feedback control of the first two modes of a flexible beam using a bridge circuit that simultaneously measured the input voltage and the mechanical strain in the material. A more detailed analysis of the electromechanical coupling was developed by Anderson *et al.* in their work on self-sensing actuation [11]. One of the detrimental aspects of the technique, "feedthrough capacitance", was noted by both groups of researchers. The work by Dosch *et al.* and Anderson *et al.* was extended by Cole and Clark through the development of an adaptive filter algorithm that identified the feedthrough capacitance of the piezoceramic sensor-actuator [12].

More recently, the concept of self-sensing has been applied to applications in active noise control. Clark and Lane developed a technique for measuring the mechanical velocity of a speaker for the purpose of making it a constant volume velocity source over a specified frequency range [13]. They demonstrated that feedback control of the mechanical velocity eliminated instabilities caused by speaker dynamics and enabled the use of pressure measurements for suppressing acoustic resonances. The technique was applied to the active suppression of acoustic resonances within a reverberant enclosure [14].

The contribution of this work is the development of a technique for simultaneously measuring the mechanical velocity and acoustic pressure. Unlike the work by Lane and Clark [13], in which only the mechanical velocity was measured for the purpose of creating a constant volume velocity source, this work utilizes the pressure measurement directly in the control algorithm. Experimental results illustrate the use of the technique for suppressing the acoustic resonances of an enclosed cavity through the use of second order feedback compensators.

2. IMPEDANCE MODELLING OF THE SPEAKER AND ACOUSTIC LOAD

The self-sensing technique is investigated with a system consisting of a cylindrical enclosure with a speaker mounted at one end. The control problem is represented by a three-mesh electromechanical impedance model, as shown in Figure 1. The relationship between the input voltage and the current across the electrical element is

$$v_{in} + (Z_e + B^2 l^2/(Z_m + A^2 Z_a) i = 0, \tag{1}$$

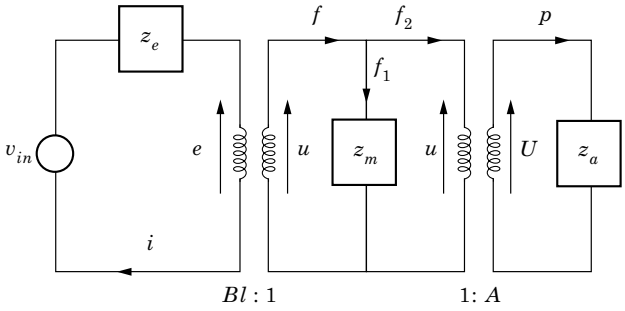

Figure 1. Electromechanical model of the speaker that incorporates the load of the acoustic element.

which illustrates that the combined impedance is a function of the electrical, mechanical, and acoustic impedances in addition to the coupling coefficients Bl and A. See the Appendix for the definitions and units associated with the elements of the impedance model. Analyzing the impedance model allows one to obtain an expression for an estimate of the mechanical velocity of the speaker:

$$\hat{u} = e/Bl = (1/Bl)(v_{in} + \hat{Z}_e\, i). \tag{2}$$

Likewise, one can define the pressure estimate as

$$\hat{p} = (1/A)(\hat{Z}_m \hat{u} + Bli). \tag{3}$$

Examining equations (2) and (3), one notes that the velocity and pressure estimates are only a function of the measured voltage and current, and the estimated mechanical and electrical impedances. No information is required about the impedance of the acoustic field. Combining these two equations yields a relationship between the input voltage and estimated pressure:

$$\hat{p}/v_{in} = (\hat{Z}_m/BlA)\{1 - (\hat{Z}_e + B^2l^2/\hat{Z}_m)1/Z_{em}\}, \tag{4}$$

where Z_{em} is the term in parentheses in equation (1). The previous expression demonstrates that the pressure estimate is the difference between the measured input voltage, v_{in}, and a filtered version of the coupled electromechanical impedance, Z_{em}.

Equation (4) illustrates the importance of the coupled electromechanical impedance in the estimate of the pressure. Rewriting the coupled impedance as

$$Z_{em} = Z_e + [(Bl)^2/Z_m]\{1/(1 + A^2Z_a/Z_m\} \tag{5}$$

one notes that in the limiting case, $|A^2Z_a| \ll |Z_m|$, the mechanical-to-acoustic coupling is approximately zero and, assuming that the electrical and mechanical impedances are estimated perfectly, equation (4) demonstrates that the pressure estimate is zero. In the general case, the amount of mechanical-to-acoustic coupling will significantly affect the ability to estimate the pressure from the current and voltage measurements of the speaker.

Consider the case of an empty cylindrical tube with a speaker mounted at one end and a rigid termination at the opposite end. Using the parameters of the experimental setup, one can plot the magnitude and phase of $(\hat{Z}_e + B^2l^2/\hat{Z}_m)$ $(1/Z_{em})$ as a function of the mechanical-to-acoustic coupling coefficient, A. Assuming that the electrical and mechanical impedances are estimated perfectly, one notes that the plot approaches 1 at all frequencies in which $|A^2Z_a| \ll |Z_m|$. Figure 2 illustrates that it becomes increasingly difficult to resolve the term $(\hat{Z}_e + B^2l^2/\hat{Z}_m)$ $(1/Z_{em})$ as the mechanical-to-acoustic coupling coefficient becomes smaller.

Two general conditions can be derived by analyzing the coupling between the electrical, mechanical, and acoustic impedances. Resolving the pressure from the electromechanical impedance Z_{em} becomes increasingly difficult as the acoustic impedance becomes small compared to the mechanical impedance. In the case in which $|A^2Z_a|$ is comparable or larger than $|Z_m|$, the combined mechanical and acoustic impedance $(B^2l^2)/(Z_m + A^2Z_a)$ must also be comparable to the electrical impedance Z_e. Thus, for a given acoustic load, the self-sensing technique derived in this paper will be most effective at frequencies in which the magnitude of the acoustic impedance is on the same order as the magnitude of the mechanical impedance and the electrical impedance is low compared to the term $(B^2l^2)/(Z_m + A^2Z_a)$.

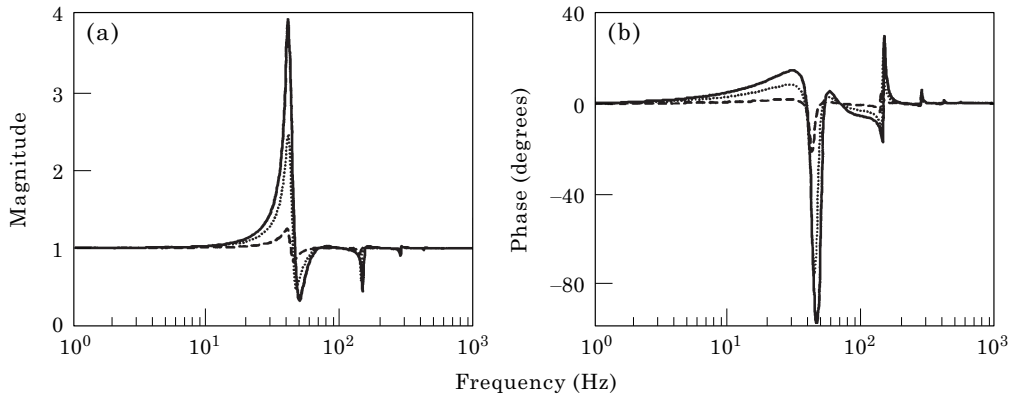

Figure 2. Variation in $(\hat{Z}_e + B^2l^2/\hat{Z}_m)$ $(1/Z_{em})$ as a function of the mechanical-to-acoustic coupling coefficient: (a) magnitude, (b) phase. Key: —, area $A = \pi r_{spkr}^2$; · · · ·, $A = \pi r_{spkr}^2/2$; - - - -, $A = \pi r_{spkr}^2/10$ (- - - -).

3. EXPERIMENTAL RESULTS

The estimation technique is experimentally tested on a cylindrical enclosure with a speaker mounted at one end. One end of the tube is essentially a rigid end condition made from plywood while a plywood enclosure containing a 6 inch diameter speaker is mounted at the opposite end (see Figure 3). An accelerometer is affixed using epoxy to the speaker cone and a microphone is placed on a bracket approximately 2 in away from the cone surface. A second microphone is placed on the outer diameter of the rigid end of the tube. The wires for these transducers are connected through the plywood enclosures to eliminate holes in the enclosed cavity.

Signal conditioning is required for the accelerometer, microphones, and current sensor. The accelerometer is a standard measurement instrument weighing 32 gs. The pressure sensors are electret condenser microphones that require a simple resistor–capacitor network for signal conditioning. Current through the speaker is measured with a differential amplifier that measures the voltage drop across a 0·61 Ω resistor. Data acquisition and control systems are used for dynamic analysis and real-time implementation of the estimation technique. An eight-channel spectral analyzer measures input–output transfer functions and a five-input, six-output digital signal processing system is used for real-time estimation and control.

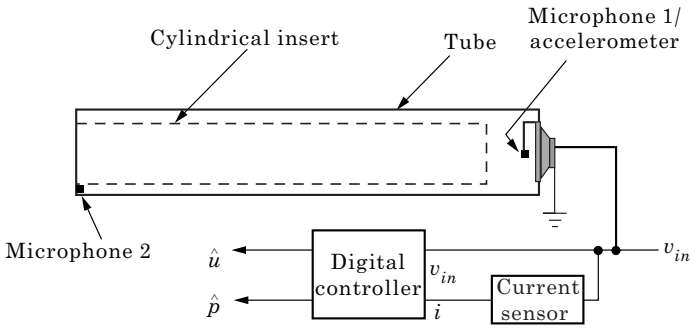

Figure 3. Experimental setup.

A cylindrical insert is placed in the enclosure to vary the dynamics of the acoustic load. The insert is constructed from plastic tubing and occupies approximately 70% of the interior volume of the enclosure. The insert has a significant effect on the natural frequencies of the interior cavity. The first and second natural frequencies of the cavity are reduced from approximately 140 Hz and 280 Hz without the insert to 100 Hz and 132 Hz with the insert.

3.1. *Impedance tests*

The first set of tests is performed on the speaker mounted outside of the enclosure and radiating into a large open room. This test is performed to determine the electromechanical impedance of the speaker for a small acoustic load. Assuming that the acoustic load is small enough such that $|A^2 Z_a| \ll |Z_m|$, the combined electrical–mechanical impedance is approximately

$$v_{in}/i \approx Z_e + (Bl)^2/Z_m. \tag{6}$$

The results of the impedance test are shown in Figure 4. As expected, the impedance is purely real at low frequencies and exhibits a peak near the mechanical resonance of the speaker. The only anomaly in the test results is the slope of the impedance magnitude at frequencies above approximately 150 Hz. A standard model for the electrical impedance of a speaker is a resistor in series with an inductor [15], which yields a high frequency slope of 1 on a log–log plot of the impedance magnitude. Curvefitting the measured data reveals that the log–log slope of the impedance magnitude is 0·602 for the speaker used in this study.

The non-integer slope exhibited by the measured data requires a change in the model of the electrical impedance. As equation (4) illustrates, the pressure estimate depends on the estimates of the electrical and mechanical impedance in addition to the coupled electromechanical impedance, Z_{em}. To maximize the accuracy of the impedance estimates, an interlaced pole-zero model of the form

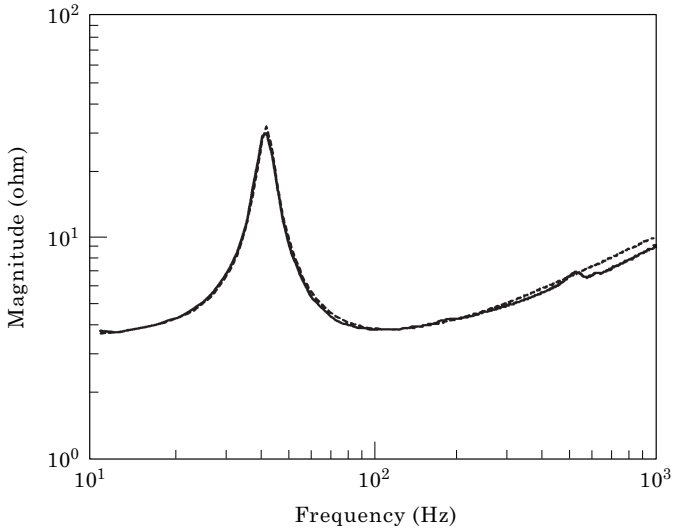

Figure 4. Measured speaker impedance radiating into an open room (—) and the magnitude of the pole-zero impedance model (- - - -).

$$\hat{Z}_e = \hat{R} \prod_{m=-N}^{N} \frac{(\hat{L}/\hat{R})\Delta^{N-m}s + 1}{(\hat{L}/\hat{R})\Delta^{N-m+\gamma/2}s + 1} \tag{7}$$

is utilized. From the standpoint of modelling the electrical impedance, a pole-zero model of this form has several beneficial characteristics. The DC gain of the system is simply $\hat{R}$ due to the form of the numerator and denominator. For $\Delta < 1$, the transfer function has a positive slope of $\gamma/2$ at high frequencies and the first transfer function zero occurs at $\omega = \hat{L}/\hat{R}$. The parameter Δ is chosen to make the transfer function estimate accurate over approximately a decade, i.e., 150–1500 Hz. With these parameters, the estimated electrical impedance is expressed by

$$\hat{Z}_e = \hat{R} \prod_{m=-5}^{5} \frac{(\hat{L}/\hat{R})(0{\cdot}691)^{5-m}s + 1}{(\hat{L}/\hat{R})(0{\cdot}691)^{5-m+1{\cdot}204}s + 1}. \tag{8}$$

A comparison of the estimated impedances and the measured values are also shown in Figure 4. The interlaced pole-zero model is able to accurately represent the high frequency behaviour of the electrical impedance.

The estimate of the mechanical impedance is developed from a mass spring damper model of the speaker cone:

$$\hat{Z}_m = (M_{md}s^2 + R_{ms}s + K_{ms})/s \tag{9}$$

Equation (9) assumes that the piston is rigid in the frequency range of interest.

3.2. *Pressure estimation*

The pressure estimation technique is tested by placing the speaker in the enclosure and comparing the estimated pressure with a direct measurement of the quantity. The equations for estimated pressure and estimated velocity are implemented in real time on a digital signal processor sampling at 28·5 kHz. The sampling rate is deemed high enough compared to the bandwidth of interest ($\approx$ 500 Hz) that the system is modelled in continuous time.

The block diagram of the digital implementation is shown in Figure 5. The current and voltage across the speaker is measured with an analog circuit and these two quantities are input to the digital signal processor. In accordance with equation (2), the velocity estimate is formed from the expression

$$\hat{u} = (1/Bl)(g_u v_{in} + \hat{Z}_e i). \tag{10}$$

The variable g_u is a gain that accounts for the error in the calibration of the current sensor. It is essentially a tuning parameter that is varied to obtain more accurate estimate of the velocity. The pressure estimate is implemented by the expression

$$\hat{p} = \hat{Z}_m \hat{u} + g_p(Bl)i, \tag{11}$$

which, again, contains a variable gain g_p to obtain a more accurate estimate of the pressure. Furthermore, to eliminate overflow in the processor, this pressure estimate does not contain the multiplicative factor $1/A$.

The pressure and velocity estimates are "tuned" by changing the values of $\hat{R}$, g_u, $\hat{L}$ and g_p. At each parameter value, the frequency response between the estimated quantities and the input voltage (i.e., $\hat{u}/v_{in}$ and $\hat{p}/v_{in}$) is compared to the frequency responses obtained with the accelerometer and microphone 1. The velocity measurement

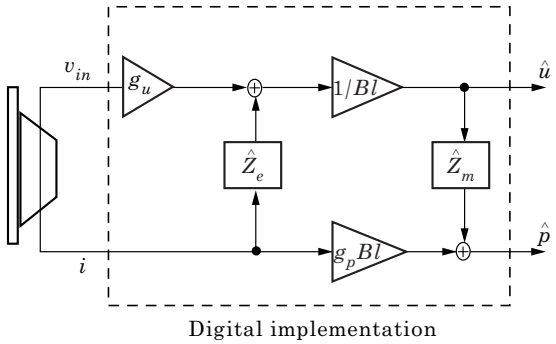

Figure 5. Block diagram of the digital implementation of the pressure and velocity estimation technique.

is obtained by dividing the acceleration response by $j\omega$, where ω is the measurement frequency in rad/s.

Experimental results indicate that the process can be broken down into two steps. First, the parameters $\hat{R}$ and g_u are chosen such that an accurate velocity estimate is obtained. The second step in the process involves varying $\hat{L}$ and g_p to obtain an accurate estimate of the pressure. It is found experimentally that accurate estimates of the velocity lead to accurate pressure estimates in the low frequency region of the response. Once $\hat{R}$ and g_u are chosen properly, the region between approximately 20 and 80 Hz is accurate in the pressure response, but the frequency region above 80 Hz is very sensitive to the choice of $\hat{L}$ and g_p.

The frequency response between the input voltage and the pressure estimates are shown in Figure 6 for the best choice of the tuning parameters. The results demonstrate that an accurate estimate of the pressure, both in magnitude and phase, is obtained over the frequency range 20–150 Hz. Above this frequency the pressure estimate deviates substantially from the actual pressure response. The deviation causes all of the acoustic resonances above 150 Hz to be unobservable in the frequency response of the pressure estimate.

The experimental results are consistent with the impedance analysis of the coupled system. Accurate measurements of the pressure response between 20 and 150 Hz are attributed to the fact that the acoustic impedance of the tube is comparable in magnitude to the mechanical impedance in this frequency range. This explains the

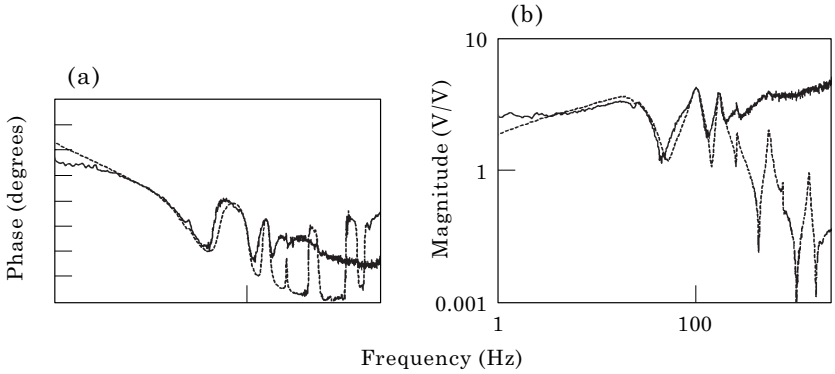

Figure 6. Pressure estimates after tuning the frequency responses (—) and the measured pressure response (- - - -): (a) phase (b) magnitude.

accurate measurement of the pressure near the peaks and the error in the pressure measurement near the zeroes of the acoustic impedance. Above 150 Hz, the errors in the pressure response are attributed to two factors. First, the acoustic impedance in this frequency range becomes smaller in magnitude compared to the mechanical impedance, thus reducing the coupling between the speaker and the acoustic load. Secondly, the electrical impedance of the speaker becomes larger in this frequency range compared to the coupled mechanical–acoustic impedance, thus making it difficult to resolve the pressure response at higher frequencies. Furthermore, the accuracy of the pressure measurement is reduced at higher frequencies due to inaccuracies in the estimate of the electrical impedance (see Figure 4). All of these factors combine to limit the bandwidth of the pressure estimate to approximately 20–150 Hz.

4. ACTIVE DAMPING OF THE ACOUSTIC RESONANCES

The use of the pressure estimate technique enables feedback control of the acoustic resonances without the need for additional sensors. A set of experiments is performed to demonstrate the effectiveness of the pressure estimation technique for active damping of the cavity resonances.

The feedback compensator is a second order filter of the form

$$K(s) = g_f \omega_f^2 / (s^2 + 2\zeta_f \omega_f \omega_f^2), \tag{12}$$

where the parameters g_f, ζ_f, and ω_f are the gain, damping ratio, and natural frequency of the control filter. This type of compensator is referred to as a positive position feedback filter and has been used previously in the control of resonant systems [16, 17]. The second order filter is implemented using the same digital signal processor used to implement the pressure and velocity estimator.

The feedback compensator is designed using the measured transfer function between the input voltage v_{in} and the pressure estimate $\hat{p}$. The gain, natural frequency and damping ratio are chosen to make the gain of the series combination of $K(s)$ and $G(s) = \hat{p}/v_{in}$ greater than one in the frequency range of the first two acoustic resonances (roughly 100–140 Hz) while maintaining low frequency stability near the speaker resonance (approximately 50 Hz).

The results of the feedback control implementation for the 70% fill factor are shown in Figure 7. The transfer functions illustrate the effect of active damping on the acoustic response at both ends of the tube. Increasing the gain of the compensator adds damping to the acoustic resonances at 100 Hz and 132 Hz. The damping in the 100 Hz mode increases from an open-loop value of 4·4% to a closed-loop value of 14·93% critical The damping in the acoustic resonance at 132 Hz increases from 2·4% critical to 3·23% critical. The acoustic response actually becomes larger near the low-frequency resonance of the speaker due to the small phase margin in the frequency response of $K(j\omega)G(j\omega)$. The small phase margin is attributed to the phase lag associated with the mechanical resonance of the speaker.

The control results illustrate the utility of the pressure estimation technique for actively suppressing interior acoustic resonances. Over the frequency range in which the pressure estimate is valid—approximately 20–150 Hz for the present tests—the pressure estimate enables active suppression of the acoustic resonances with rather simple feedback compensators. The simplicity of the feedback compensation and the robustness of the estimation technique is advantageous for systems in which the interior acoustic resonances are uncertain or time varying.

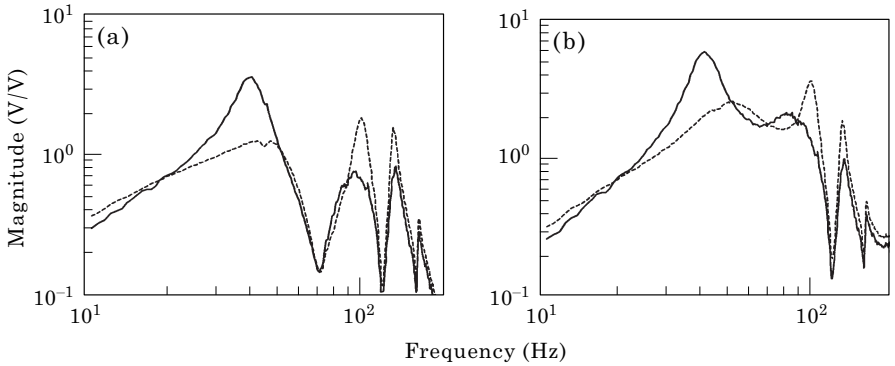

Figure 7. Open-loop (- - - -) and closed-loop (—) feedback control results utilizing the pressure estimate: (a)

5. CONCLUSIONS

A "self-sensing" technique was developed for estimating the mechanical velocity and acoustic pressure from the measurement of speaker voltage and current. The technique was derived from an impedance model that incorporated the electrical and mechanical dynamics of the speaker in addition to the dynamics of the coupled acoustic field. The advantage of the technique is that it allows the measurement of acoustic pressure without the need for additional sensors.

The estimation technique was demonstrated on a enclosure that consisted of a closed cylindrical tube with a speaker mounted at one end. The current and voltage of the speaker were measured with an analog circuit and the pressure and velocity estimator was implemented digitally. The estimates of the speaker resistance, inductance, and mechanical impedance were determined from measured transfer functions. Experimental results indicated that an accurate pressure estimated could be obtained over the frequency range 20–150 Hz. Errors in the pressure estimate at frequencies greater than 150 Hz were attributed to the weak mechanical-to-acoustic coupling and imperfect estimation of the electrical impedance.

Active damping of the acoustic resonances was demonstrated on the tube with the cylindrical enclosure. A second order feedback compensator was implemented to add active damping to the first two acoustic resonances. Experimental results demonstrated that feedback control increased the damping in the 100 Hz mode from 4·4% critical to 14·9% critical, while the damping in the second acoustic resonance increased from 2·4% critical 3·2% critical. The small phase margin near the mechanical resonance of the speaker caused an increase in the acoustic response in the 25–50 Hz frequency range. Future work will concentrate on increasing the bandwidth of the pressure estimate and eliminating the detrimental effects of the mechanical resonance in the closed-loop response.

ACKNOWLEDGMENTS

This work was supported by the 1998 Summer Faculty Research sponsored by the Air Force Office of Scientific Research. The authors would like to thank their focal points,

Dr. Steven Griffin and Dr. Dino Sciulli of the Dynamics Branch of the AFRL Phillips Site, for supporting this summer research. The first author would also like to thank the Mechanical, Industrial, and Manufacturing Engineering Department of the University of Toledo for their support during the research phase of this program.

REFERENCES

1. H. F. Olson and E. G. May 1953 *Journal of the Acoustical Society of America* **25**, 1130–1136. Electronic sound absorber.
2. W. B. Conover 1956 *Noise Control* **2**, 78–82. Fighting noise with noise.
3. P. A. Nelson and S. J. Elliot 1992 *Active Control of Sound*. London: Academic Press.
4. S. J. Elliot, I. M. Stothers, P. A. Nelson, A. M. McDonald, D. C. Quinn and T. Saunders 1988 In *Proceedings of the Inter-Noise Conference* 987–990. The active control of engine noise inside cars.
5. S. J. Elliot, P. A. Nelson, I. M. Stothers and C. C. Boucher 1990 *Journal of Sound and Vibration* **140**, 219–238. In-flight experiments on the active control of propeller-induced cabin noise.
6. P. A. Nelson and S. J. Elliot 1987 *Journal of Theoretical and Applied Mechanics Supplement* **6**, 39–98. Active minimization of acoustic fields.
7. P. A. Nelson, A. R. D. Curtis, S. J. Elliot, and A. J. Bullmore 1987 *Journal of Sound and Vibration* **117**, 1–13. The active minimization of harmonic enclosed sound fields, part: theory.
8. S. J. Elliot, P. Joseph, P. A. Nelson and M. E. Johnson 1991 *Journal of the Acoustical Society of America* **90**, 2501–2512. Power output minimization and power absorption in the active control of sound.
9. F. Orduna-Bustamante and P. A. Nelson 1992 *Journal of the Acoustical Society of America*, **91**, 2740–2747. An adaptive controller for active absorption of sound.
10. J. Dosch, D. J. Inman and E. Garcia 1992 *Journal of Intelligent Material Systems and Structures* **3**, 166–185. A self-sensing piezoelectric actuator for collocated control.
11. E. H. Anderson, N. Hagood and J. M. Goodliffe 1992 *AIAA Paper Number* 92-2465-CP. Self-sensing piezoelectric actuation: analysis and application to controlled structures.
12. D. G. Cole and R. L. Clark 1995 *Journal of Intelligent Material Systems and Structures* **5**, 665–672. Adaptive compensation of piezoelectric sensoriactuators.
13. S. A. Lane and R. L. Clark 1997 submitted to the *Journal of the Audio Engineering Society*. Improving loudspeaker performance for active noise control applications.
14. S. A. Lane and R. L. Clark 1998 In *Proceedings of the American Control Conference* 2606–2610. Active control of a reverberant enclosure using an approximate constant volume velocity source.
15. L. L. Beranek 1954 *Acoustics*. New York: McGraw-Hill.
16. D. J. Leo and D. J. Inman 1993 *Smart Materials and Structures Journal* **2**, 82–95. Modeling and control simulations of slewing flexible frame containing active members.
17. J. L. Dosch, D. J. Leo and D. J. Inman 1995 *Journal of Guidance, Control, and Dynamics* **18**, 340–346. Modeling and control for vibration suppression of a flexible active structure.

APPENDIX : NOMENCLATURE

v_{in}	speaker input voltage (V)
i	speaker current (A)
e	voice coil back emf (V)
R	electrical resistance (Ω)
L	electrical inductance (H)
z_a	acoustic mobility (m^5/N s)
z_m	mechanical mobility (m/N s)

Z_e	electrical impedance (Ω)
Z_a	acoustic impedance (N s/m^5)
Z_m	mechanical impedance (N s/m)
f, f_1, f_2	mechanical force (N)
p	acoustic pressure (N/m^2)
u	speaker velocity (m/s)
U	volume velocity (m^3/s)
A	speaker area (m^2)
Bl	voice coil force factor (Wb/m)
M_{md}	speaker moving mass (kg)
R_{ms}	speaker damping coefficient (N s/m)
K_{ms}	speaker stiffness (N/m)